THE TOPOLOGY OF SURFACE SKIN FRICTION AND VORTICITY FIELDS IN WALL-BOUNDED FLOWS

M.S. Chong
Department of Mechanical Engineering
The University of Melbourne
Victoria 3010 AUSTRALIA
min@unimelb.edu.au

J.P. Monty and I. Marusic
Department of Mechanical Engineering
The University of Melbourne
Victoria 3010 AUSTRALIA

ABSTRACT

In previous studies, the three invariants of the velocity gradient tensor have been used to study turbulent flow structures. For incompressible flow the first invariant P is zero and the topology of the flow structures can be investigated in terms of the second and third invariants, Q and R respectively. However, these invariants are zero at a no slip wall and can no longer be used to identify and study structures at the surface in a wall-bounded flow. At the wall, the flow field can be described by a no slip Taylor-series expansion. Like the velocity gradient tensor, it is possible to define the invariants $\mathscr{P}$, $\mathscr{Q}$ and $\mathscr{R}$ of the no slip tensor. In this paper it will be shown how the topology of the flow field on a no slip wall can be studied in terms of these invariants.

INTRODUCTION

A critical point is a point in a flow field where the velocity $u_1 = u_2 = u_3 = 0$ and the streamline slope is indeterminate. Close to the critical point the velocity field can be described by the linear terms of a Taylor-series expansion. Two types of critical points can be described: one is the free slip critical point which is located away from a no slip wall and the other is the no slip critical point which occurs on a no slip wall.

Free-slip critical points

For free slip critical points, the velocity u_i in x_i space is given by

$$\begin{bmatrix} u_1 \\ u_2 \\ u_3 \end{bmatrix} = \begin{bmatrix} \dot{x_1} \\ \dot{x_2} \\ \dot{x_3} \end{bmatrix} = \begin{bmatrix} dx_1/dt \\ dx_2/dt \\ dx_3/dt \end{bmatrix} = \begin{bmatrix} A_{11} & A_{12} & A_{13} \\ A_{21} & A_{22} & A_{23} \\ A_{31} & A_{32} & A_{33} \end{bmatrix} \begin{bmatrix} x_1 \\ x_2 \\ x_3 \end{bmatrix}$$

or

$$\dot{x_i} = \frac{dx_i}{dt} = A_{ij} x_j \tag{1}$$

where $A_{ij} = \partial u_i / \partial x_j$ is the velocity gradient tensor.

The invariants of the velocity gradient tensor

For an observer moving in a non-rotating frame of reference with any particle in a flow field, the flow surrounding the particle is described in terms of the nine components of the velocity gradient tensor A_{ij}.

The characteristic equation of A_{ij} is

$$\lambda_i^3 + P\lambda_i^2 + Q\lambda_i + R = 0, \tag{2}$$

where λ_i are the eigenvalues and P, Q and R are the tensor invariants which are defined as

$$\begin{aligned} P &= -(A_{11} + A_{22} + A_{33}) \\ Q &= A_{11}A_{22} - A_{12}A_{21} + A_{11}A_{33} - A_{13}A_{31} \\ &\quad + A_{22}A_{33} - A_{23}A_{32} \qquad \text{and} \\ R &= A_{11}A_{23}A_{32} - A_{11}A_{22}A_{33} + A_{12}A_{21}A_{33} \\ &\quad - A_{12}A_{23}A_{31} - A_{13}A_{21}A_{32} + A_{13}A_{22}A_{31} \end{aligned} \tag{3}$$

The characteristic equation (2) can have (i) all real roots which are distinct, (ii) all real roots where at least two roots are equal, or (iii) one real root and a conjugate pair of complex roots. In the $P-Q-R$ space, the surface which divides the real solutions from the complex solutions is given by

$$27R^2 + (4P^3 - 18PQ)R + (4Q^3 - P^2Q^2) = 0 \tag{4}$$

For incompressible flow, the first invariant P is zero and hence all free-slip critical points can be described by the second and third invariants, i.e. Q and R respectively. The invariants

of the velocity gradient tensor have been used to study turbulent flow structures in order to extract information regarding the scales, kinematics and dynamics of these structures (see Davidson, 2004, pg. 268 and Elsinga & Marusic, 2010). These invariants can also be used to study turbulent structures using data from Direct Numerical Simulations (DNS), for example in the DNS of homogeneous isotropic turbulence by Ooi et al. (1999) and in wall-bounded shear flows by Chong et al. (1998).

No slip critical points

In wall-bounded flows, there is no slip at the wall, i.e. $u_1 = u_2 = u_3 = 0$ when $x_3 = 0$, where x_3 is the wall-normal direction. If the origin of a Taylor-series expansion is located on the no slip wall, i.e. at $x_3 = 0$, the linear terms of the expansion are given by

$$\begin{bmatrix} u_1 \\ u_2 \\ u_3 \end{bmatrix} = \begin{bmatrix} 0 & 0 & A_{13} \\ 0 & 0 & A_{23} \\ 0 & 0 & 0 \end{bmatrix} \begin{bmatrix} x_1 \\ x_2 \\ x_3 \end{bmatrix}$$

where $A_{13} = \partial u_1/\partial x_3$ and $A_{23} = \partial u_2/\partial x_3$; x_1 is the streamwise direction and x_2 is the spanwise direction. All the invariants of the above tensor are zero at the wall and hence they cannot be used to map the topology of the flow pattern at a no slip surface.

To satisfy the no slip condition, the Taylor-series expansion at the wall (i.e. at $x_3 = 0$) can be re-written to include higher order terms and at the same time satisfy the no slip boundary condition. The expansion is given by

$$\begin{aligned} u_1 &= A_{13}x_3 + (\mathscr{A}_{11}x_1 + \mathscr{A}_{12}x_2 + \mathscr{A}_{13}x_3)x_3 \\ u_2 &= A_{23}x_3 + (\mathscr{A}_{21}x_1 + \mathscr{A}_{22}x_2 + \mathscr{A}_{23}x_3)x_3 \\ u_3 &= \qquad\quad (\mathscr{A}_{31}x_1 + \mathscr{A}_{32}x_2 + \mathscr{A}_{33}x_3)x_3 \end{aligned}$$

Since $u_1 = u_2 = u_3 = 0$ at the wall (at $x_3 = 0$), we cannot integrate the velocity field at the wall to obtain the surface flow pattern or skin friction lines. However, by defining $\overset{o}{x}_i$ as

$$\overset{o}{x}_i = \frac{dx_i}{d\tau} \tag{5}$$

where $d\tau = x_3 dt$. the no slip velocity field can be expressed as

$$\begin{aligned} \frac{u_1}{x_3} &= \overset{o}{x}_1 = \frac{dx_1}{d\tau} = A_{13} + (\mathscr{A}_{11}x_1 + \mathscr{A}_{12}x_2 + \mathscr{A}_{13}x_3) \\ \frac{u_2}{x_3} &= \overset{o}{x}_2 = \frac{dx_2}{d\tau} = A_{23} + (\mathscr{A}_{21}x_1 + \mathscr{A}_{22}x_2 + \mathscr{A}_{23}x_3) \\ \frac{u_3}{x_3} &= \overset{o}{x}_3 = \frac{dx_3}{d\tau} = \qquad (\mathscr{A}_{31}x_1 + \mathscr{A}_{32}x_2 + \mathscr{A}_{33}x_3) \end{aligned}$$

A critical point occurs on the wall when $A_{13} = A_{23} = 0$ and at this critical point

$$\begin{bmatrix} \overset{o}{x}_1 \\ \overset{o}{x}_2 \\ \overset{o}{x}_3 \end{bmatrix} = \begin{bmatrix} dx_1/d\tau \\ dx_2/d\tau \\ dx_3/d\tau \end{bmatrix} = \begin{bmatrix} \mathscr{A}_{11} & \mathscr{A}_{12} & \mathscr{A}_{13} \\ \mathscr{A}_{21} & \mathscr{A}_{22} & \mathscr{A}_{23} \\ \mathscr{A}_{31} & \mathscr{A}_{32} & \mathscr{A}_{33} \end{bmatrix} \begin{bmatrix} x_1 \\ x_2 \\ x_3 \end{bmatrix}$$

or

$$\overset{o}{x}_i = \frac{dx_i}{d\tau} = \mathscr{A}_{ij}x_j. \tag{6}$$

In this paper, the $\mathscr{A}_{ij}$ will be referred to as the 'no slip tensor'. The above vector field can be integrated with τ to generate surface streamlines (limiting streamlines or skin friction lines).

The invariant of the no slip tensor

To satisfy boundary conditions on a no slip surface, the no slip tensor is given by

$$\mathscr{A}_{ij} = \begin{bmatrix} \mathscr{A}_{11} & \mathscr{A}_{12} & \mathscr{A}_{13} \\ \mathscr{A}_{21} & \mathscr{A}_{22} & \mathscr{A}_{23} \\ 0 & 0 & -\frac{1}{2}(\mathscr{A}_{11} + \mathscr{A}_{22}) \end{bmatrix} \tag{7}$$

By substitution of the above expansion into the Navier-Stokes equation, it can be shown that $\mathscr{A}_{11}$, $\mathscr{A}_{12}$, $\mathscr{A}_{21}$ and $\mathscr{A}_{22}$ are related to the vorticity gradients and $\mathscr{A}_{13}$ and $\mathscr{A}_{23}$ are related to pressure gradients. Like the velocity gradient tensor, the no slip tensor has three invariants $\mathscr{P}$, $\mathscr{Q}$ and $\mathscr{R}$. For incompressible flow, the first invariant $\mathscr{P}$ is no longer zero and is given by

$$\mathscr{P} = -\frac{1}{2}(\mathscr{A}_{11} + \mathscr{A}_{22}). \tag{8}$$

It can also be shown that the relationship between the three invariants of the no slip tensor is given by

$$2\mathscr{P}^3 + \mathscr{P}\mathscr{Q} + \mathscr{R} = 0. \tag{9}$$

SURFACE SKIN FRICTION AND SURFACE VORTICITY VECTOR FIELDS

The main aim of this study is to investigate the topology of skin friction fields and the surface vorticity field at the wall in wall-bounded flows. Wall shear stress or skin friction is defined as the normal derivative of the velocity vector at the wall. Hence the direction of the near-wall velocity vector when projected normal to the wall is in the same direction as the wall shear stress vector, i.e. surface streamlines are known as skin friction lines. Figure 1 shows skin friction lines in a streamwise-spanwise plane at the no slip wall using data from the Direct Numerical Simulation (DNS) of channel flow by del Alamo et al. (2004). The simulation is for $Re_\tau = hu_\tau/\nu = 934$ where h is the channel half height, ν is the kinematic viscosity and u_τ is the friction velocity.

Skin friction lines (limiting streamlines at the no slip wall) are obtained from integrating the streamwise velocity u_1 and spanwise velocity u_2 in the first plane from the wall, and it generally assumed that this first plane is very close to the wall. How close this plane has to be to produce sufficiently accurate skin friction lines, is an open debatable issue. In most computations of wall bounded flows it is generally

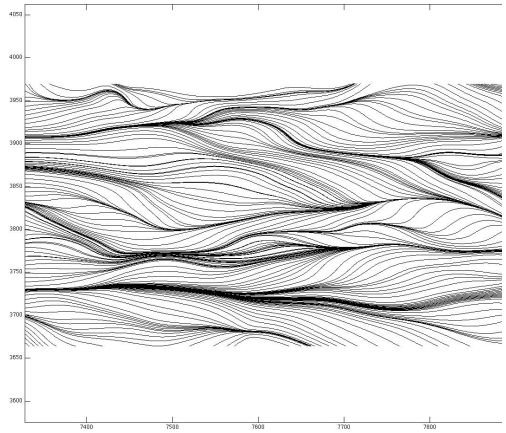

Figure 1. Typical surface skin friction lines at the wall using data from DNS of channel flow at $Re_\tau = 934$ (see del Alamo et al., 2004 for details of computations). The region shown is for a random area of the entire channel wall in the computational domain.

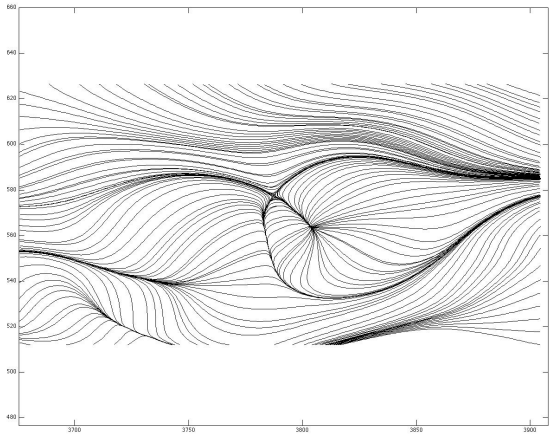

Figure 2. Surface skin friction field showing critical points (a saddle and a node) at the wall from the same data as that in figure1.

agreed that the first plane is such that $x_3^+ = x_3 u_\tau/\nu \leq 1$. In the computation by del Alamo et al. (2004), the first plane off the wall is for $x_3^+ = 0.0313$. The surface skin friction lines shown in figure 1 are for a small region of the flow, i.e. for $x_1^+ \times x_2^+ \, plane \approx 300 \times 925$, the size of the entire streamwise-spanwise channel wall, in viscous units, is 3072×2304 . The figure is fairly typical of surface skin friction lines which consist of bifurcation lines which are associated with surface streak lines and streamwise vortical motions (or streamwise eddying motions) at the wall.

A question this study seeks to answer is: Are there critical points in the surface skin friction field?

This question is best addressed by considering the surface vorticity lines which are orthogonal to the surface skin friction lines (see Chong et al., 1998). It is conjectured in the DNS of wall bounded flows, that since the flow is periodic in the spanwise direction and the outflow is re-cycled

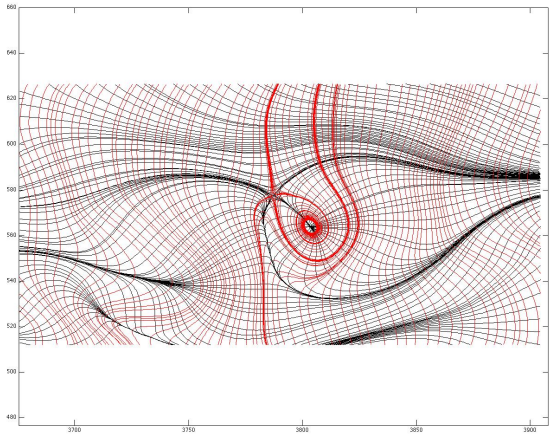

Figure 3. Surface vortex lines (red) superimposed on the surface skin friction field shown in figure 2. Surface vortex lines are orthogonal to the surface skin friction lines. Note that critical points in the surface skin friction field are also critical points in the surface vorticity field. A saddle in the skin friction field is also a saddle in the vorticity field. A node in the skin friction field is a focus in the vorticity field.

and fed back as inflow, the surface skin friction field at the no slip wall can be mapped on to the surface of a toroid. The Poincare-Hopf index theorem or Poincare Bendixson theorem (see Hunt, et al., 1978, Lighthill, 1963 or Flegg, 1974) states that the topology of a smooth vector field on a toroidal surface is such that the number of nodes minus the number of saddles is equal to zero, a saddle having a Poincare index of -1 and a node (or a focus) having a Poincare index of +1. Hence, if the skin friction field for the entire no slip wall is similar to that shown in figure 1, where no critical points can be seen, then the Poincare-Hopf index theorem is satisfied. This led to the initial conclusion that there are probably no critical points on the surface of a no slip wall since a single critical point (a single saddle or a single node) will violate the Poincare-Hopf theorem for the topology of the flow field on the surface of a toroidal surface.

However, contrary to expectations, there are critical points in the surface skin friction field at the wall. Figure 2 shows a close-up ($x_1^+ \times x_2^+ \, plane \approx 100 \times 225$) from another area of a surface skin friction field using data from the same computation as that used to produce figure 1. This figure shows an example of critical points which are found to exist on the no slip wall; these critical points come as a saddle-node pair so that the Poincare index around the pair of critical points is such that it is zero around a closed circuit enclosing the two critical points. Critical points in the surface skin friction field are also critical points in the surface vorticity field. In fact, all critical points on the surface come as a saddle-node pair so that for the entire surface in the computational domain, the Poincare-Hopf index theorem is satisfied. The topology of the surface vorticity field also satisfies the condition that the surface vortex lines must form closed loops and can only cross at critical points in vorticity. Critical points can also be found on the surface using data from the DNS of a pipe flow by Chin et al. (2010) and also in the recent spatial computation of a zero pressure gradient turbulent boundary layer by Wu &

Moin (2009).

Taylor-series expansion solutions of the Navier-Stokes equations

To investigate the three-dimensional structure of the flow on a no slip surface, the technique described in Perry & Chong (1986) will be used to generate smooth three-dimensional skin friction vector fields which are local solutions of the Navier-Stokes equations. The velocity field for a complex flow can be represented by Taylor-series expansions of arbitrary order N as

$$u_i = \sum_{n=0}^{N} S(a_i,b_i,c_i) x_1^{a_i} x_2^{b_i} x_3^{c_i} \tag{10}$$

where $i = 1,2,3$, and x_i are the orthogonal spatial coordinates. (a_i,b_i,c_i) uniquely specify the terms in the expansion and the powers of x_1, x_2 and x_3 respectively.

The factor[1] S is given by

$$S = \frac{(a_i+b_i+c_i)!}{a_i!b_i!c_i!} \tag{11}$$

and

$$n = a_i+b_i+c_i \tag{12}$$

The above representation of the expansion for the velocity field is ideal for generating algorithms so that computer programs can be written to obtain Taylor-series expansion for the velocity, to arbitrary orders. Once generated, the expansions in the above notation can be translated to a more conventional notation. For example, the third order Taylor-series expansion for the streamwise velocity u_1, in a conventional notation, is given by

$$\begin{aligned} u_1 &= P_1 + P_2x_1 + P_3x_2 + P_4x_3 \\ &+ P_5x_1^2 + P_6x_2^2 + P_7x_3^2 + 2P_8x_1x_2 + 2P_9x_1x_3 \\ &+ 2P_{10}x_2x_3 + P_{11}x_1^3 + P_{12}x_2^3 + P_{13}x_3^3 + 3P_{14}x_1^2x_2 \\ &+ 3P_{15}x_1^2x_3 + 3P_{16}x_1x_2^2 + 3P_{17}x_1x_3^2 + 3P_{18}x_2^2x_3 \\ &+ 3P_{19}x_2x_3^2 + 6P_{20}x_1x_2x_3 \end{aligned} \tag{13}$$

where the P's are the coefficients of the Taylor expansion. The expansion for the spanwise velocity u_2 and the wall normal velocity u_3 are similar to the above expansion, except that the coefficients are denoted by $Q's$ and $R's$ respectively[2].

It can be shown that the number of unknown coefficients for a N^{th}-order expansion is given by

$$N_c = 3\sum_{K=0}^{N}\sum_{J=0}^{K+1} J \tag{14}$$

The Navier-Stokes equation and continuity equation in tensor notation[3] is given by

$$\frac{\partial u_i}{\partial t} + u_j\frac{\partial u_i}{\partial x_j} = -\frac{\partial p}{\partial x_i} + \nu\frac{\partial^2 u_i}{\partial x_j \partial x_j} \tag{15}$$

$$\frac{\partial u_i}{\partial x_i} = 0 \tag{16}$$

where p is 'kinematic' pressure $= p/\rho$ and ν is the kinematic viscosity.

Differentiating the velocity expansions (13), substitution into the continuity equation (16), and equating like powers of x_1, x_2 and x_3, relationships between the coefficients can be generated. Examples of continuity relationships generated from equation (16) are:

$$\begin{aligned} P_2 + Q_3 + R_4 &= 0 \\ P_5 + Q_8 + R_9 &= 0 \\ P_8 + Q_6 + R_{10} &= 0 \\ \text{...} \quad &\text{etc} \end{aligned} \tag{17}$$

For an N^{th}-order expansion, the number of these relationships is given by

$$E_c = \sum_{n=0}^{N}\sum_{J=0}^{n} J \tag{18}$$

By equating cross-derivatives of pressure in the Navier-Stokes equations, and by collecting terms for like powers of x_1, x_2 and x_3, the Navier-Stokes relationships can be generated. A typical example of a Navier-Stokes relationship for a fifth order expansion is given below:

$$\begin{aligned} \dot{R_8} - \dot{P_{10}} \\ +R_2P_8 + R_3Q_8 + R_4R_8 + R_5P_3 + R_6Q_2 \\ +R_8P_2 + R_8Q_3 + R_9R_3 + R_{10}R_2 + 3R_{14}P_1 \\ +3R_{16}Q_1 + 3R_{20}R_1 - P_2P_{10} - P_3Q_{10} - P_4R_{10} \\ -P_6Q_4 - P_7R_3 - P_8P_4 - P_9P_3 - P_{10}Q_3 \\ -P_{10}R_4 - 3P_{18}Q_1 - 3P_{19}R_1 - 3P_{20}P_1 \\ -12\nu(R_{24} + R_{26} + R_{35} - P_{33} - P_{28} - P_{29}) = 0 \end{aligned} \tag{19}$$

For an N^{th}-order expansion, the number of these relationships is given by

$$E_{NS} = \sum_{n=3}^{N}\sum_{J=2}^{n-1}(2J-1) \tag{20}$$

Note that for time-dependent flow, these relationships are ordinary differential equations (hence determining the dynamics of the flow). For steady flow problems these relationships,

[1] S was introduced in the original technique for generating the Taylor-series expansions and is retained in the analysis given in this paper - for details, see Perry & Chong (1986).

[2] Note that P's, Q's and R's are coefficients of the expansion for the velocity field and not to be confused with the invariants of the velocity gradient tensor.

[3] Using Einstein's notation where repeated indices implies summation over indices 1, 2 and 3.

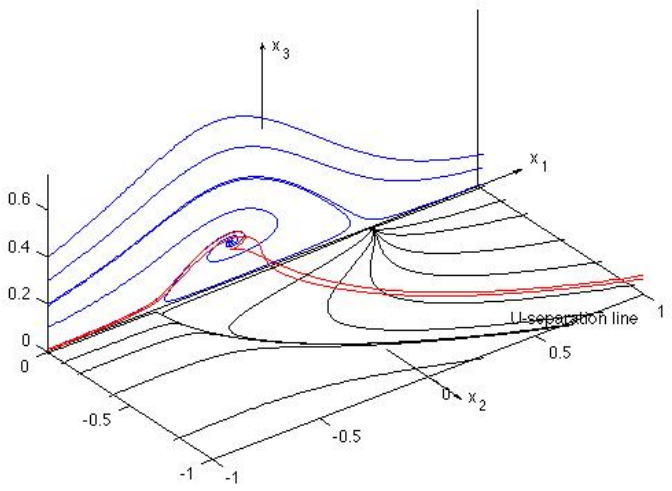

Figure 4. Local three-dimensional separation pattern. Flow is in the x_1 direction. $x_1 - x_2$ is the no slip surface and $x_1 - x_3$ is a plane of symmetry.

like the continuity relationships, are algebriac (kinematic) relationships.

The number of unknown coefficients for different order expansions and the number of continuity and Navier-Stokes relationships generated is given in the following table.

N	N_c	E_c	E_{NS}
0	3	0	0
1	12	1	0
2	30	4	0
3	60	10	3
4	105	20	11
5	168	35	26
.	.	.	.
.	.	.	.
15	2448	680	1001

In all cases the total number of relationships generated exceeds the total number of unknown coefficients of a given order expansion N, and hence further equations are needed for closure.

Three-dimensional separated flow on a no slip wall

A third order solution for separated flow above a no-slip surface will be used to illustrate how a solution can be generated.

Applying the no-slip condition (all coefficients without x_3 are zero) and continuity, the third-order Taylor-series expansions for the velocity field given in (13) expansion are reduced to

$$\begin{aligned} u_1 &= P_4 x_3 + P_7 x_3^2 + 2P_9 x_1 x_3 + 2P_{10} x_2 x_3 + P_{13} x_3^3 \\ &+ 3P_{15} x_1^2 x_3 + 3P_{17} x_1 x_3^2 + 3P_{18} x_2^2 x_3 + 3P_{19} x_2 x_3^2 \\ &+ 6P_{20} x_1 x_2 x_3 \\ u_2 &= Q_4 x_3 + Q_7 x_3^2 + 2Q_9 x_1 x_3 + 2Q_{10} x_2 x_3 + Q_{13} x_3^3 \\ &+ 3Q_{15} x_1^2 x_3 + 3Q_{17} x_1 x_3^2 + 3Q_{18} x_2^2 x_3 + 3Q_{19} x_2 x_3^2 \\ &+ 6Q_{20} x_1 x_2 x_3 \end{aligned}$$

$$\begin{aligned} u_3 &= R_7 x_3^2 + R_{13} x_3^3 + 3R_{17} x_1 x_3^2 + 3R_{19} x_2 x_3^2 \end{aligned} \tag{21}$$

To further simplify the problem, the flow is assumed to be symmetrical about the $x_1 - x_3$ plane, i.e. u_1 is even in x_2, hence $P_{10} = P_{19} = P_{20} = 0$ and u_2 is odd in x_2, hence $Q_4 = Q_7 = Q_9 = Q_{13} = Q_{15} = Q_{17} = Q_{18} = 0$. From continuity

$$R_{19} = -(P_{20} + Q_{18}) = 0$$

and the expansions simplify to

$$\begin{aligned} u_1 &= P_4 x_3 + P_7 x_3^2 + 2P_9 x_1 x_3 + P_{13} x_3^3 \\ &+ 3P_{15} x_1^2 x_3 + 3P_{17} x_1 x_3^2 + 3P_{18} x_2^2 x_3 \\ u_2 &= 2Q_{10} x_2 x_3 + 3Q_{19} x_2 x_3^2 + 6Q_{20} x_1 x_2 x_3 \\ u_3 &= R_7 x_3^2 + R_{13} x_3^3 + 3R_{17} x_1 x_3^2 \end{aligned} \tag{22}$$

The above expansion has to satisfy continuity, i.e.

$$\begin{aligned} P_9 + Q_{10} + R_7 &= 0 \\ P_{15} + Q_{20} + R_{17} &= 0 \\ P_{17} + Q_{19} + R_{13} &= 0 \end{aligned} \tag{23}$$

For a steady solution of the Navier-Stokes equation,

$$R_{17} - P_{15} - P_{18} - P_{13} = 0 \tag{24}$$

The no-slip velocity field is given by

$$\begin{aligned} \overset{o}{x_1} = u_1/x_3 &= P_4 + P_7 x_3 + 2P_9 x_1 + P_{13} x_3^2 \\ &+ 3P_{15} x_1^2 + 3P_{17} x_1 x_3 + 3P_{18} x_2^2 \\ \overset{o}{x_2} = u_2/x_3 &= 2Q_{10} x_2 + 3Q_{19} x_2 x_3 + 6Q_{20} x_1 x_2 \\ \overset{o}{x_3} = u_3/x_3 &= R_7 x_3 + R_{13} x_3^2 + 3R_{17} x_1 x_3 \end{aligned} \tag{25}$$

Further equations can be generated by specifying the location and properties of critical points in the flow field. For example, in generating a separated flow pattern, the properties of separation/reattachment points can be expressed as

$$\begin{bmatrix} \overset{o}{x_1} \\ \overset{o}{x_2} \\ \overset{o}{x_3} \end{bmatrix} = \begin{bmatrix} a & 0 & B \\ 0 & na & 0 \\ 0 & 0 & -\frac{1}{2}a(n+1) \end{bmatrix} \begin{bmatrix} x_1 \\ x_2 \\ x_3 \end{bmatrix} \tag{26}$$

For an angle of separation/separation θ, B is given by

$$B = \frac{-\frac{1}{2}a(n+3)}{tan\theta} \tag{27}$$

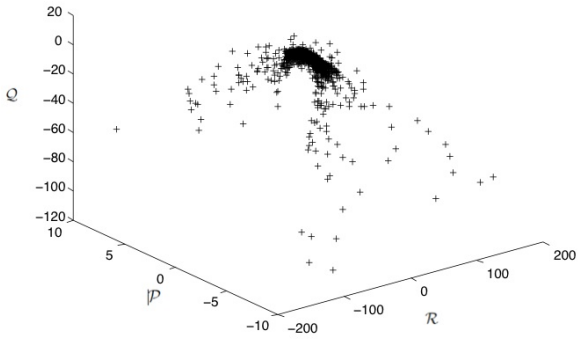

Figure 5. The invariants of the no slip tensor for the DNS of channel flow.

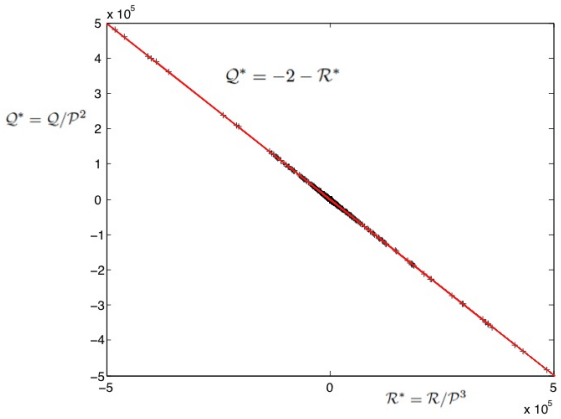

Figure 6. The invariants of the no slip tensor normalised (see equation (9)).

Using a few simple parameters, various three-dimensional flow patterns can be generated. Figure 4 shows the local surface skin friction field, consisting of a saddle-node pair, which is similar to the topology of the skin friction field around critical points found on the wall in the DNS of wall bounded flows. Figure 4 also shows the three-dimensional structure above the surface (in the $x_1 - x_3$ plane) indicating the saddle-node pairs are the footprints of local three-dimensional separated flow at the surface, caused by local vorticity and pressure gradients. Although one would expect that the flow structures to be two dimensional on the surface, the above study shows that the structures at the surface are three dimensional. However, these instantaneous local vortical structures are exceedingly small and the significance of these structures and effects on turbulent structures further from the wall has yet to be investigated. In an incompressible flow, vorticity is only generated at the no-slip wall. Many questions remained unanswered, for example: Is local instantaneous flow separation necessary for the creation of three-dimensional vortical structures at the wall?

The invariants of the no slip tensor at the wall may also be used to help lead to a further understanding of flow structures at the wall. Figure 5 is a scatter plot showing the distribution of the three no slip invariants for the channel flow simulation of del Alamo et al. and figure 6 shows that the second and third invariants can be normalized as indicated by equation (9). These two normalized invariants can be used to describe structures on the surface of a no slip wall in a wall bounded flow simulation. How these invariants are related to the topological structures (critical points) in the surface skin friction and surface vorticity fields is the subject of future work in this study of near wall structures in wall bounded flows.

CONCLUSION

A initial study of the topological structure of the surface skin friction field and surface vorticity field is described in this paper. The importance of these local structures on much larger mean flow structures found in turbulent wall bounded flows has yet to be fully investigated.

ACKNOWLEDGEMENTS

The authors will like to acknowledge the use of data from various DNS of wall bounded flows. This work is funded by ARC Grant DP1093585.

REFERENCES

[1] Chin, C., Ooi, A.S.H., Marusic, I., and Blackburn, H., 2010, The influence of pipe length on turbulence statistics computed from direct numerical simulation data. *Phys. Fluids* **22**, 115107, 1-10.

[2] Chong, M.S., Soria, J., Perry, A.E., Chacin, J., Cantwell, B.J. and Na, Y., 1998, Turbulence structures of wall-bounded shear flows found using DNS data. *J. Fluid Mech.*, **357**:225-247.

[3] Davidson P.A. *Turbulence* Oxford University Press. 2004.

[4] Elsinga, G.E. and Marusic, I. , 2010, Evolution and lifetimes of flow topology in a turbulent boundary layer. *Physics of Fluids*, **22**, 2010, 015102.

[5] Hunt, J.C.R., Abell, C.J., Peterka, J.A., Woo, H., 1987, Kinematic studies of the flows around free or surface-mounted obstacles; applying topology to flow visualization. *J. Fluid Mech.*, **86**:179-200.

[6] Lighthill, M.J., 1963, Attachment and separation in three-dimensional flow. In *Laminar Boundary Layers*, ed. L. Rosenhead, pp. 72-82. Oxford: Oxford University Press.

[7] Flegg, G.C., 1974, *From Geometry to Topology.* English Universities Press.

[8] Ooi, A., Chong, M.S. and Soria, J., 1999, A study of the invariants associated with the velocity gradient tensor in homogeneous flows. *J. Fluid Mech.*, **381**:141-174.

[9] Perry, A.E. and Chong, M.S., 1987, A description of eddying motions and flow patterns using critical-point concepts. *Ann. Rev. Fluid Mech.*, **19**:125-155.

[10] Perry, A.E. and Chong, M.S., 1986, A series-expansion study of the Navier-Stokes equations with application to three-dimensional separation patterns. *J. Fluid Mech.*, **173**:207-223.

[11] Wu, Xu. and Moin, P., 2009, Direct numerical simulation of turbulence in a nominally zero-pressure-gradient flat-plate boundary layer. *J. of Fluid Mech.*, **630**:5-41.